

江陵凹陷西南部始新世盐湖卤水演化和钾锂来源 ——来自石盐流体包裹体的证据

颜开^{1,2}, 王春连¹, 陈仁义¹, 刘雪^{1,3}, 刘延亭^{1,4}, 尹传凯¹, 孙珮婕^{1,5},
赵雨欣^{1,5}, 廖世龙^{1,6}

(1. 中国地质科学院矿产资源研究所, 自然资源部成矿作用与资源评价重点实验室, 北京 100037; 2. 冰岛大学地球科学学院, 雷克雅未克 102; 3. 昆明理工大学国土资源工程学院, 云南昆明 650093; 4. 东华理工大学地球科学学院, 江西南昌 330013; 5. 成都理工大学沉积地质研究院, 四川成都 610059; 6. 长江大学地球物理与石油资源学院, 湖北武汉 430100)

摘要: 江陵凹陷中部和北部发现了富钾锂卤水的存在, 而西南部地区则以不含钾锂的固体蒸发岩为主。本次研究旨在通过ZK0303井石盐流体包裹体中的化学成分来揭示凹陷西南部古盐湖卤水的演化和钾锂的来源。根据镜下观察, 在始新世的3个石盐层中找到了具有人字形和堆积形的原生流体包裹体, 并利用激光剥蚀电感耦合等离子体质谱仪(LA-ICP-MS)技术测试了石盐单个原生流体包裹体中Li、K、Mg、Ca、Br的浓度。通过实验数据的分析, 凹陷西南部始新世石盐流体包裹体中卤水为Na-K-Mg-Ca-Cl型, 其中K的浓度最高达到3 362.15 mg/L, Li的浓度最高达到15.10 mg/L。ZK0303井3组石盐层中Mg-Ca-2K之间的关系表明, 凹陷西南部盐湖卤水达到钾石盐沉积阶段。3个石盐组中各离子浓度的变化说明, 盐湖卤水的蒸发程度经历了由低升高再降低的变化。根据前人的研究, 卤水中钾锂的来源与凹陷内的玄武岩密切相关。但是凹陷西南部地区离玄武岩分布区较远难以获得足够的物质补给, 该地区始新世盐湖卤水中的钾锂元素除蒸发外, 还可能来源于早期岩盐的溶解。

关键词: 江陵凹陷; 石盐原生流体包裹体; 钾石盐沉积; 岩盐溶解

中图分类号: P619.21⁺¹

文献标识码: A

文章编号: 1000-6524(2024)-0905-13

The evolution of Eocene saline lake brine and sources of K and Li in the southwestern Jiangling depression: Evidence from fluid inclusion of halite

YAN Kai^{1,2}, WANG Chun-lian¹, CHEN Ren-yi¹, LIU Xue^{1,3}, LIU Yan-ting^{1,4}, YIN Chuan-kai¹,
SUN Pei-jie^{1,5}, ZHAO Yu-xin^{1,5} and LIAO Shi-long^{1,6}

(1. MNR Key Laboratory of Metallogeny and Mineral Assessment, Institute of Mineral Resources, Chinese Academy of Geological Sciences, Beijing 100037, China; 2. Institute of Earth Sciences, University of Iceland, Reykjavík 102, Iceland; 3. Faculty of Land Resource Engineering, Kunming University of Science and Technology, Kunming 650093, China; 4. School of Earth Sciences, East China University of Technology, Nanchang 330013, China; 5. Institute of Sedimentary Geology, Chengdu University of Technology, Chengdu 610059, China; 6. College of Geophysics and Petroleum Resources, Yangtze University, Wuhan 430100, China)

Abstract: The potassium and lithium-rich brine is found in the central and northern part of Jiangling depression,

收稿日期: 2023-11-03; 接受日期: 2024-01-09; 编辑: 尹淑苹

基金项目: 国家重点研发计划(2023YFC2906605); 国家自然科学基金(U20A2092, 41502089); 中国地质调查局地质调查项目(DD20230056, DD20190437, DD20190606); 中央级公益性科研院所基本科研业务费专项(KK2005, KK2016)

作者简介: 颜开(1992-), 男, 博士后, 研究方向为盐湖卤水钾锂矿床成矿, E-mail: yankai_ytq@sina.com; 通讯作者: 王春连(1983-), 男, 研究员, 主要从事非金属矿产成矿理论研究, E-mail: wangchunlian312@163.com。

网络首发时间: 2024-01-17; 网络首发地址: <http://kns.cnki.net/kcms/detail/11.1966.P.20240115.1642.002.html>

while the southwest area is dominated by solid evaporites without potassium and lithium. This study aims to investigate the evolution of the paleo-saline lake brine in the southwestern Jiangling depression and sources of K and Li by the chemical composition of halite fluid inclusions of well ZK0303. Microscopic observations revealed the presence of primary fluid inclusions with chevron and cumulate structures in three groups of halite layers. The concentrations of Li, K, Mg, Ca, Br from the individual primary fluid inclusions were analyzed using laser ablation inductively coupled plasma mass spectrometry (LA-ICP-MS). According to the analysis of experimental data, the brine of Eocene halite fluid inclusion in the southwestern of the Jiangling depression is Na-K-Mg-Ca-Cl type, in which the highest concentration of K is 3 362.15 mg/L, and the highest concentration of Li is 15.10 mg/L. The relationship between Mg-Ca-2K of three halite layers in well ZK0303 shows that the brine of Eocene saline lake in the southwestern depression reached the stage of sylvite precipitation. The changes of each ion concentration of the three halite layers show that the degree of evaporation of Eocene saline lake had changed from low to high and then decreased. According to previous studies, the sources of Li and K in the brine are closely related to the basalt in the depression. However, the southwest area of the depression is far from the basalt distribution area, and it is difficult to obtain sufficient material supply. Lithium and K of the Eocene saline lake brine in this area may come from the dissolution of early halite in addition to evaporation.

Key words: Jiangling depression; primary fluid inclusion of halite; sylvite precipitation; dissolution of halite

Fund support: National Key Research and Development Project of China (2023YFC2906605); National Natural Science Foundation of China (U20A2092, 41502089); Project of China Geological Survey (DD20230056, DD20190437, DD20190606); Central Welfare Basic Scientific Research Business Expenses (KK2005, KK2016)

晚白垩世-古近纪期间,受构造运动的影响,在华南地区形成了一系列的裂谷盆地,如江汉盆地、洞庭盆地、清江与吉泰盆地等。以上湖盆在晚白垩世-古近纪时期大多演化为盐湖,并沉积了巨量石盐岩等盐类矿产(刘庆民等,1982;储澄,1983;方志雄,2006;姚秋昌等,2008;王春连等,2020)。其中,在江汉盆地发现深层卤水,富含钾、锂、硼、铷、铯、溴、碘等新兴战略型矿产资源,其品位已达到工业利用或综合利用水平(刘成林,2013;王春连等,2013a,2015,2021)。经过多年的找钾工作,王春连等(2013b)、刘成林(2013)、沈立建等(2014)、刘锦磊等(2015)通过研究蒸发岩层中含钾矿物及地球化学特征,认为江汉盆地江陵凹陷古新统至下始新统为主要的富钾层位,成钾条件好,具有开发前景。江陵凹陷卤水主要分布于凹陷的北部,与古近纪火山岩分布区域重合,而在凹陷西南部仅发现了硬石膏、钙芒硝及石盐等不含钾的蒸发岩矿物。因此,本次研究以江陵凹陷西南部古近纪始新统新沟嘴组原生石盐包裹体为研究对象,通过激光剥蚀技术(LA-ICP-MS)恢复古盐湖化学组成,并深入探究盐湖卤水演化过程以及钾锂的来源,为江陵凹陷南北卤水分布存在差异提供合理解释。

石盐矿物里原生流体包裹体内保存着沉积时残

余的水圈和大气中的物质,蕴藏着大量的原始地质信息,因此可以获得关于水温、水化学甚至是形成蒸发岩的大气条件的详细信息(Roberts and Spencer, 1995; Benison and Goldstein, 1999; 刘兴起等, 2005; 王春连等, 2013a; 董娟等, 2015; 席斌斌等, 2015; 徐洋等, 2018, 2021; Xu et al., 2021a)。但是石盐、钾石盐等蒸发岩矿物作为一种特殊的沉积产物,具有易溶、难保存的特点。后期的改造和破坏作用(如成岩作用、构造活动等)常常导致蒸发岩沉积地层中捕获的原始地质信息大量流失,从而影响人们对蒸发岩沉积环境及成盐机理做出正确的判断(赵艳军等, 2016)。因此,在分析测试化学组成前,需要对石盐流体包裹体开展精细的矿物学和岩相学研究,保证所测试的样品能反映原始的地质信息。目前针对石盐流体包裹体成分分析的方法主要有:激光剥蚀电感耦合等离子体质谱法(LA-ICP-MS)(Shepherd et al., 1998, 2000; Ghazi and Stephen, 2000; 孙小虹等, 2016)、微钻-超微分析法(Petrychenko et al., 2005; Kovalevych et al., 2006)、低温冷冻扫描电镜-能谱法(Timofeeff et al., 2001, 2006; Lowenstein et al., 2001)以及显微拉曼光谱法(Frezzotti et al., 2012)。其中,激光剥蚀电感耦合等离子质谱(LA-ICP-MS)可以对直径大于20 μm的单个石盐流

体包裹体进行原位、多元素同时检测,而且具有高灵敏度、低检出限等优点。在国内,Sun等(2013)首次将该方法应用于盐类矿物流体包裹体原位成分研究,成功获得了新疆罗布泊古盐湖卤水的化学信息;Xu等(2021b)通过该方法对新疆库车盆地始新世盐湖卤水化学组分进行了还原。因此,本次研究将利用激光剥蚀电感耦合等离子体质谱仪(LA-ICP-MS)对江汉盆地西南部ZK0303井始新世石盐原生流体包裹体化学成分进行分析,旨在揭示江陵凹陷南部盐湖卤水的演化以及为钾锂元素的来源提供理论依据。

1 区域地质背景

江汉盆地($29^{\circ}26' \sim 31^{\circ}37' N$; $111^{\circ}14' \sim 114^{\circ}36' E$)位于中国的湖北省,面积约 $36\,360\text{ km}^2$,是典型的陆相裂谷盆地(图1, Gilder *et al.*, 1991; 余心起等, 2003; Teng *et al.*, 2019)。江汉盆地的构造格局受北部秦岭-大别造山带、南部江南-雪峰造山

带和西北部黄陵地块的控制和影响(Shen *et al.*, 2012; Wu *et al.*, 2017)。晚白垩世-古近纪,太平洋板块回撤引起的上地幔活跃上升流和印-亚大陆碰撞推动盆地裂陷运动的发生,导致盆地多期裂陷,形成了广泛的硅质碎屑沉积、蒸发岩和大量玄武岩流(Liu *et al.*, 2004; Li *et al.*, 2015a, 2015b; Wu *et al.*, 2020)。其中,古新统沙市组由石膏岩、钙芒硝岩、岩盐、灰褐色和棕红色泥岩、薄层粉砂岩和砂岩以及少量白云岩和玄武岩组成,卤水赋存于由砂岩和玄武岩组成的层位中(王春连等, 2018)。下始新统新沟嘴组分为上、下两部分,下段主要由灰色泥岩、粉砂岩、砂岩和岩盐、钙芒硝岩、石膏岩组成,上段为棕色泥岩、砂岩组成,卤水储存在下段砂岩或裂缝性泥岩中(Yu *et al.*, 2021)。为了确定江汉盆地新生代地层的年龄,徐论勋等(1995)和彭头平等(2006)根据玄武岩K-Ar和 ^{39}Ar - ^{40}Ar 的年代学,认为沙市组地质年龄为 $65.0 \sim 56.0\text{ Ma}$,新沟嘴组($56.0 \sim 47.0\text{ Ma}$)底部是古新世与始新世的分界线。

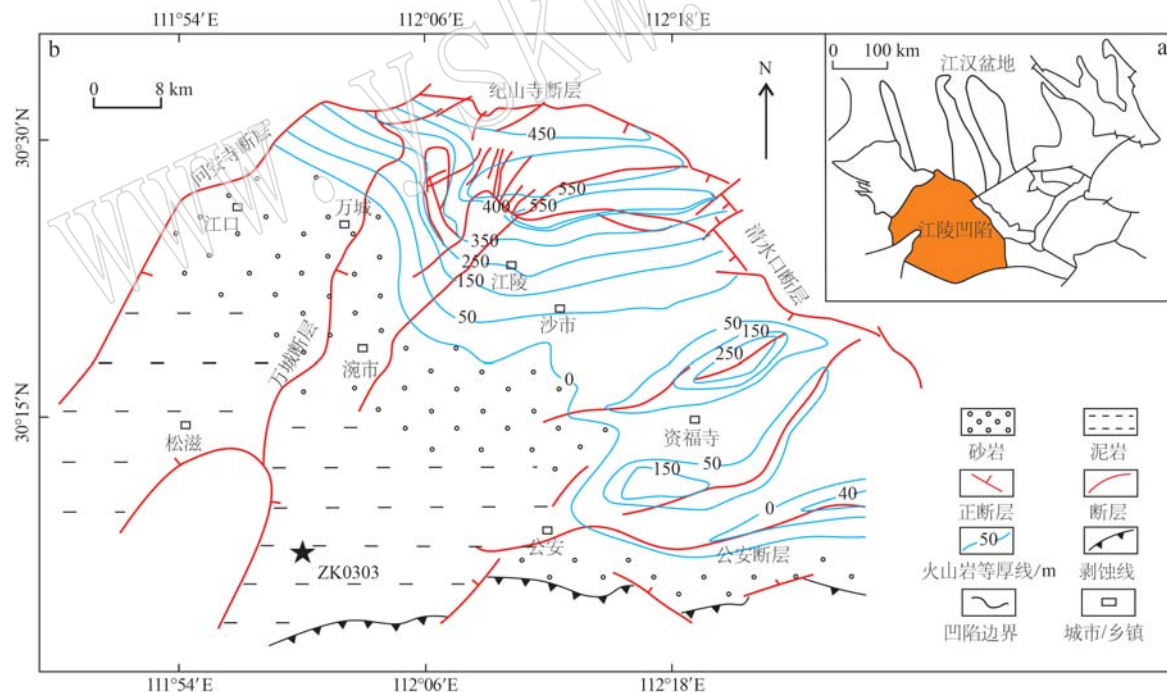


图1 江陵凹陷地质构造简图(据 Yu *et al.*, 2021)

Fig. 1 Geological structure diagram of the Jiangling depression (modified after Yu *et al.*, 2021)

江汉盆地由十多个次级凹陷组成,其中以西南部的江陵凹陷最大(图1a)。ZK0303井作为一口科研钻探井,位于江陵凹陷的西南部(图1b),预计钻遇地层为上白垩统渔阳组、古新统沙市组和始新统新沟嘴组,钻探深度约2 300 m。其中,ZK0303井

320~1 000 m段自下向上可划分为浅-半深咸水湖相($1\,000 \sim 680\text{ m}$)、深盐湖相($680 \sim 410\text{ m}$)和浅-滨湖相($410 \sim 320\text{ m}$)。浅-半深咸水湖相岩性以泥岩、粉砂岩为主,含层状硬石膏;深盐湖相下部为层状泥岩,上部为泥岩和蒸发岩互层;浅-滨湖相岩性

以泥岩和粉砂岩为主,蒸发岩含量极少。根据现有孢粉学记录和邻井地层对比研究,初步认为古新世与始新世界线在岩芯 680 m 左右处(Yan et al., 2022)。

2 样品采集与分析方法

ZK0303 井石盐层的分布见图 2,采样时应保证每个岩盐层段均有 2~3 个代表性的样品。将挑选出来的样品放入盛有干燥剂的样品袋中后送入实验室,并开展后续处理工作。在开展化学成分测试实验前,为避免磨片过程中破坏岩盐流体包裹体,首先选取晶型较好的岩盐,用小刀片顺解理面切开,获得厚度约 0.5~1 mm 的石盐解理片,然后在显微镜下进行岩相学观察。

ZK0303 井中符合解理片制备以及原生流体包裹体特征的样品有 9 个,位于 3 个石盐层中(图 2)。为满足激光剥蚀实验的要求,还需保证每个样品中存在尺寸大于 30 μm 的单个流体包裹体。根据以上要求挑选出石盐解理片,在镜下对其进行绘图和摄影,之后放入密封袋中并置于干燥器内保存,以便后续上机测试的进行(图 3)。

石盐原生流体包裹体成分的分析实验在中国地质科学院国家地质实验测试中心完成。电感耦合等离子质谱仪的型号是德国 Finnigan 公司生产的 Element 2,激光器为 New Wave 公司的 UP213 型,激光波长为 213 nm,脉冲宽度为 4 ns。在激光剥蚀采样条件下,以高纯氦气作为剥蚀物质的载气,用于优化剥蚀和传输效率。激光采样过程为点剥蚀模式,单个信号获取时间为 90 s,激光射击控制在 60 次/min。在进行剥蚀采样前,遮挡激光束使激光能量达到稳定,并进行 15 s 的空白计数,之后对样品中的点位进行 60 s 的连续剥蚀。在完成剥蚀采样后,用氦气继续吹扫进样系统 15 s。

实验结果的校正采用内标-外标结合法,其原理是:假设标准样品和实验对象中各元素间的相对灵敏度保持不变,根据标准元素和测试元素变化的一致性进行校正(Longerich et al., 1996; 胡明月等, 2008; Sun et al., 2013)。其中,外标法:将配置好的标准溶液吸入纯石英毛吸管中,并快速使用环氧树脂胶将其封口,粘在玻璃片上以待测试;内标法:在室温下,根据理论值计算,饱和食盐水中 Na 含量约为 141.62 g/L。因此,以石盐流体包裹体内的 Na

作为内标元素。具体的内标-外标结合法校正计算公式见胡宇飞等(2021)。

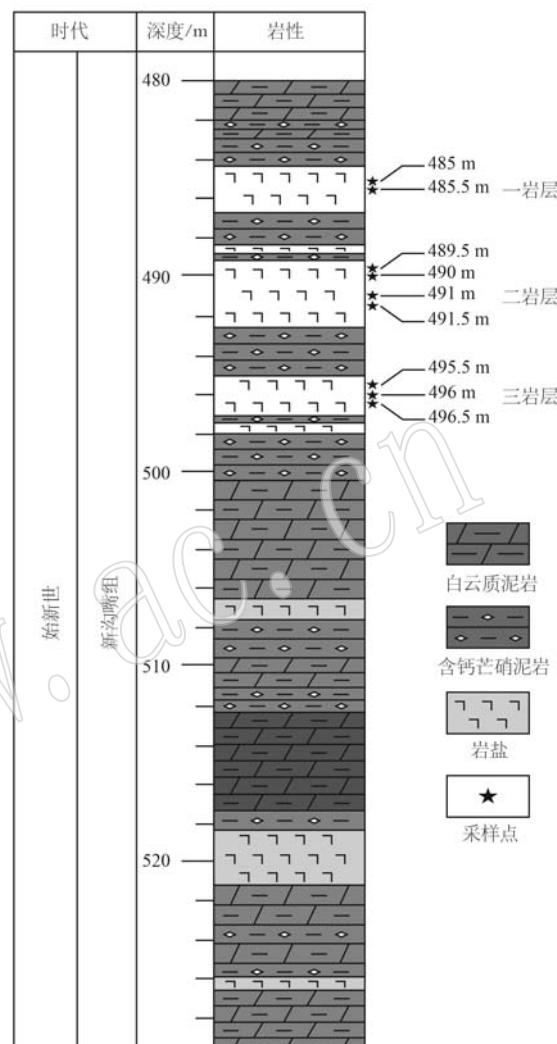


图 2 ZK0303 井石盐包裹体采样点

Fig. 2 Sampling positions of the halite fluid inclusion in well ZK0303

3 结果

3.1 包裹体化学成分

本次测试选取了 6 个石盐样品,每个样品设置了 30 个测试点,共测量 66 个流体包裹体的成分组成(图 3,表 1)。

在石盐流体包裹体成分分析测试中,包裹体内各离子信号强度随时间的推移有着不同的变化情况,以测试点位 1-5、4-4、4-17、6-17 样品为例(图 4)。在刚开始的 15 s 时间里,为使激光能量达到稳定状态,激光束被遮挡,此时激光信号表现出强度代表着

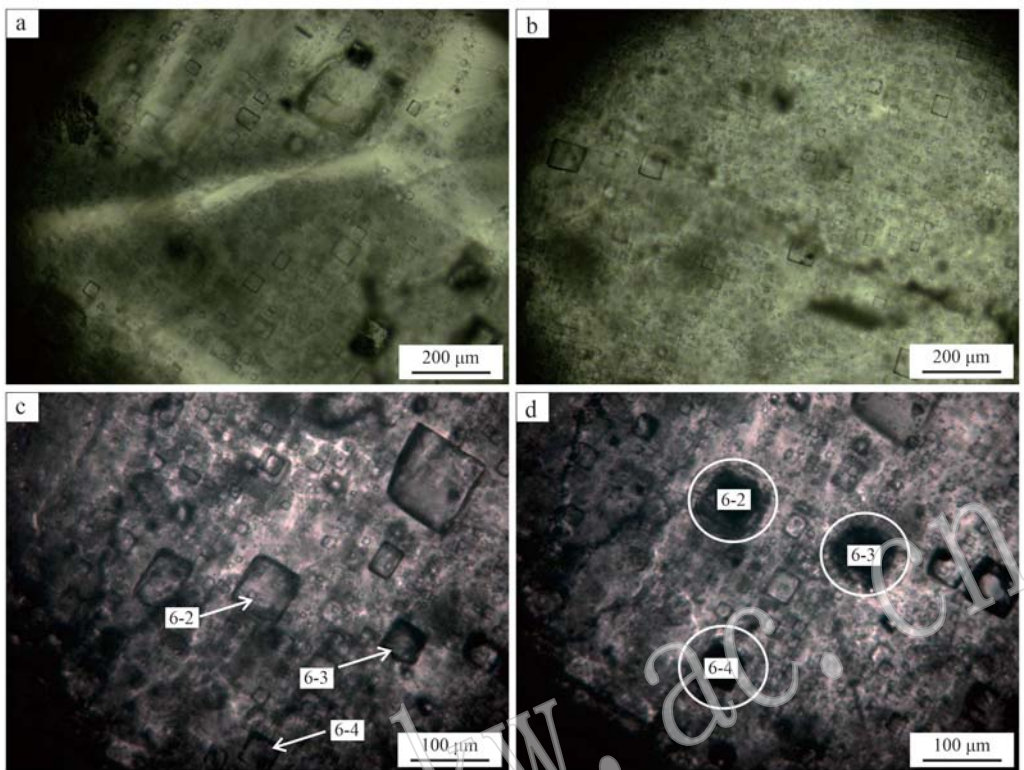


图3 ZK0303井人字形(a)、堆积形(b)和激光剥蚀前后原生石盐流体包裹体照片(c, d)
Fig. 3 Figures of chevron (a), cumulate (b) crystals and before and after the laser ablation (c, d) of primary fluid inclusions of halite, in the well ZK0303

背景强度,Na、K、Mg 和 Ca 等主量元素的信号强度十分平稳,而 Li 和 Br 微量元素的信号强度有所波动。随后激光开始对流体包裹体进行剥蚀测试,根据包裹体和石盐表面之间的距离不同,激光的信号强度会出现两种情况:①包裹体位于石盐表面。钠和其他离子的信号强度一起上升(图 4a, 4d);②包裹体和石盐表面有一定的距离。此时先发生变化的是钠离子的信号强度,有明显的强度上升,之后其他离子的信号强度开始上升(图 4b, 4c),在流体包裹体成分被激光剥蚀后,各离子信号强度迅速下降,回归到最初的背景强度。

测试的 6 个石盐样品来自于 3 个不同深度的盐层(图 2),其中 485 m 和 485.5 m 的样品来自同一石盐层,489.5 m 和 491.5 m 的样品来自同一石盐层,496 m 和 496.5 m 的样品来自同一石盐层。因此,将 6 个石盐样品由上至下分为 3 组,并统计出 3 组石盐流体包裹体中各离子浓度的均值(表 2)。

第 1 组: 485 m 样品中 Li 的均值为 1.94 mg/L,Mg 的均值为 205.13 mg/L,K 的均值为 1 050.13 mg/L,Ca 的均值为 218.09 mg/L,Br 的均值为 33.20 mg/L;485.5 m 样品中 Li 的均值为 1.05 mg/L,Mg 的均值为

141.74 mg/L,K 的均值为 489.50 mg/L,Ca 的均值为 209.30 mg/L,Br 的均值为 22.09 mg/L。

第 2 组: 489.5 m 样品中 Li 的均值为 15.10 mg/L,Mg 的均值为 1 448.54 mg/L,K 的均值为 3 362.15 mg/L,Ca 均值为 139.07 mg/L,Br 的均值为 98.58 mg/L;491.5 m 样品中 Li 的均值为 6.85 mg/L,Mg 的均值为 725.97 mg/L,K 的均值为 2 168.44 mg/L,Ca 的均值为 417.34 mg/L,Br 的均值为 35.33 mg/L。

第 3 组: 496 m 样品中 Li 的均值为 4.66 mg/L,Mg 的均值为 344.47 mg/L,K 的均值为 1 104.09 mg/L,Ca 的均值为 201.04 mg/L,Br 的均值为 49.82 mg/L;496.5 m 样品中 Li 的均值为 0.85 mg/L,Mg 的均值为 170.95 mg/L,K 的均值为 864.59 mg/L,Ca 的均值为 82.59 mg/L,Br 的均值为 9.82 mg/L。

4 讨论

4.1 原生石盐流体包裹体

作为一种易溶矿物,石盐极易随保存环境的物理化学条件的变化而发生溶解、碎裂、重结晶和变形等现象(袁见齐等,1991;杨吉根,1994),这将使得石盐

mg/L

表1 江陵凹陷ZK0303井石盐流体包裹体成分
Table 1 Compositions of halite fluid inclusions in the well ZK0303 from the Jiangling depression

深度/m	编号	Li	Mg	K	Ca	Br	深度/m	编号	Li	Mg	K	Ca	Br
485	1-5	1.14	67.36	1 051.16	88.94	8.70	4.4	4.78	632.62	2 915.52	609.10	37.07	
	1-7	1.76	259.11	599.54	151.62	34.59	4.6	1.58	209.05	473.44	257.02	19.60	
	1-9	3.29	311.14	1 643.39	299.13	47.01	4.8	1.06	488.04	381.25	146.46	14.19	
	1-11	1.55	273.82	1 510.63	268.21	76.65	4-14	8.75	1 740.25	2 482.28	479.65	48.33	
	1-12	1.98	227.65	1 263.95	283.43	23.83	4-15	17.66	830.04	3 158.77	456.17	75.10	
	1-16	0.16	53.91	679.53	136.13	2.66	491.5	4-17	9.07	889.91	2 427.16	461.76	34.39
	1-19	0.85	199.09	1 010.70	317.94	35.83		4-18	7.24	425.12	2 610.26	281.76	16.64
	1-20	1.66	116.59	720.73	213.74	31.94		4-20	7.15	900.72	3 640.42	809.62	45.19
	1-24	1.59	204.01	504.95	151.66	22.25		4-25	7.46	600.04	2 031.15	277.89	26.15
	1-26	1.66	186.44	727.82	201.03	33.01		5-1	2.12	155.85	796.16	119.86	22.89
	1-30	5.71	357.29	1 839.00	287.17	48.71		5-2	1.88	229.29	1 052.45	135.18	39.15
485.5	2-2	1.27	145.30	669.25	231.45	32.11	5-3	4.45	393.83	1 153.47	270.51	61.57	
	2-6	1.60	139.45	463.66	280.42	12.07	5-4	3.41	439.06	1 044.43	300.95	45.87	
	2-7	1.39	287.69	509.82	294.04	30.35	5-7	1.31	74.36	331.92	81.33	10.36	
	2-8	2.35	296.49	652.59	515.76	46.00	5-9	1.69	254.57	558.20	141.56	36.28	
	2-9	0.39	42.58	309.96	37.57	3.35	496	5-11	1.54	184.42	282.08	32.76	5.54
	2-11	0.84	217.55	1 054.44	213.79	39.40		5-14	8.36	297.53	978.27	88.07	24.03
	2-16	1.17	147.74	465.51	195.48	13.06		5-17	8.57	543.29	3 338.78	344.51	102.41
	2-20	0.74	81.66	191.88	238.16	23.43		5-18	3.42	361.57	1 386.55	265.24	100.42
	2-22	0.48	61.17	161.52	80.15	5.22		5-21	2.55	416.32	1 318.60	409.84	43.12
	2-23	1.17	128.04	438.68	213.05	14.41		5-23	2.78	366.84	606.23	200.93	38.00
	2-25	0.56	52.89	682.45	65.15	33.38		5-25	10.58	467.72	1 730.10	191.31	45.99
	2-27	0.66	100.34	274.2	144.54	12.24		5-28	12.63	637.94	880.07	232.48	121.88
489.5	3-1	40.26	3 539.71	8 572.42	158.09	267.97	6-1	0	459.05	1 217.22	107.39	29.63	
	3-2	9.16	932.07	2 386.47	135.89	56.50	6-3	1.53	134.79	487.48	46.43	6.28	
	3-3	6.19	1 174.25	2 460.17	118.23	34.42	6-4	2.01	364.93	1 445.07	78.07	12.82	
	3-5	4.16	512.76	2 063.59	58.04	22.15	6-5	0.83	89.61	380.64	39.59	5.22	
	3-6	3.05	460.37	1 190.50	45.53	31.18	496.5	6-7	0.49	86.54	435.47	72.69	6.08
	3-7	33.90	2 207.52	4 073.61	397.99	125.30		6-10	0	38.48	1 666.00	197.27	1.23
	3-8	10.70	919.84	2 691.28	227.17	101.85		6-12	0.56	83.59	348.06	42.75	5.75
	3-9	23.01	2 255.88	3 976.09	71.10	106.9		6-14	0.40	149.05	498.49	103.28	10.05
	3-11	5.48	1 034.45	2 845.20	39.62	140.96		6-16	0.93	90.70	823.67	80.43	10.10
	491.5	4.2	3.74	493.88	1 564.10	393.92	36.66	6-17	1.74	212.79	1 343.83	57.97	11.06

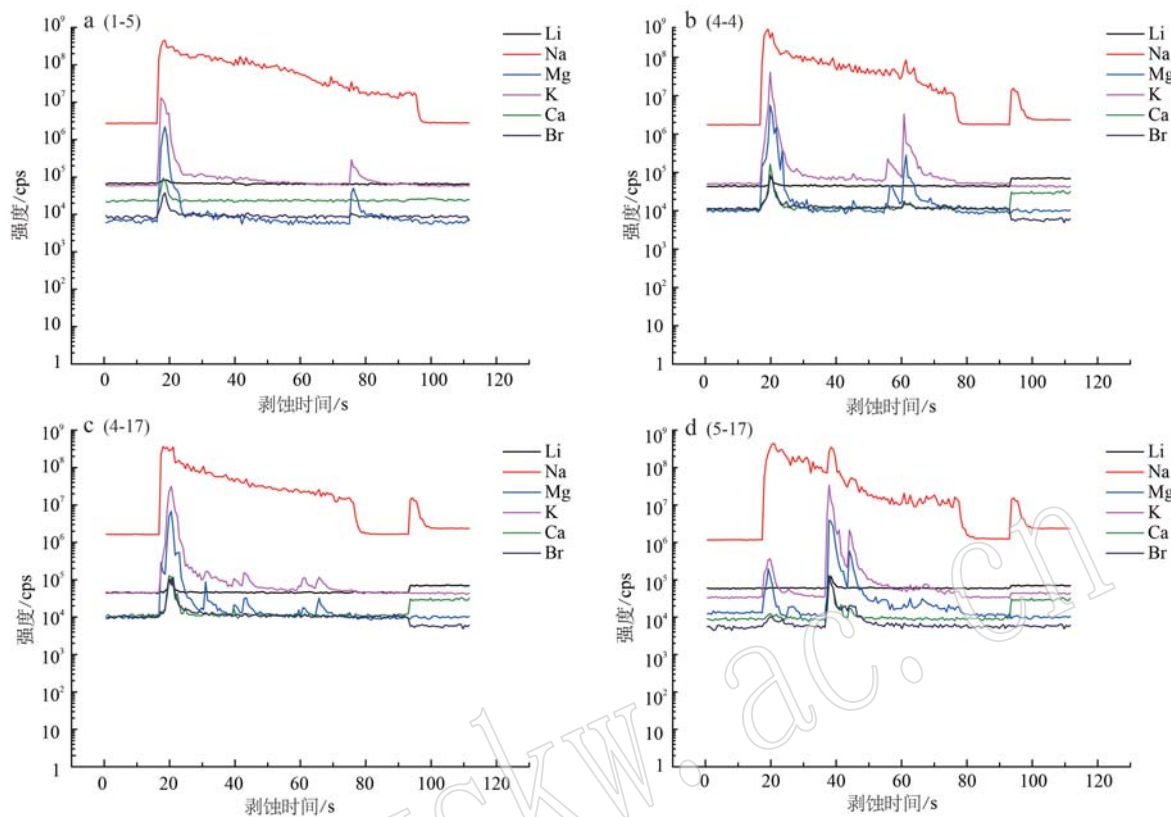


图4 石盐单个流体质谱信号强度随时间的变化

Fig. 4 Mass spectrum signal intensity vs. time for the single fluid inclusion in halite

表2 ZK0303井石盐流体包裹体化学成分平均值 mg/L

Table 2 Average chemical composition of fluid inclusions from halite in well ZK0303

深度/m	石盐组	Li	Mg	K	Ca	Br
485	1	1.94	205.13	1 050.13	218.09	33.20
485.5		1.05	141.74	489.50	209.30	22.09
489.5	2	15.10	1 448.54	3 362.15	139.07	98.50
491.5		6.85	725.97	2 168.44	417.34	35.33
496	3	4.66	344.47	1 104.09	201.04	49.82
496.5		0.85	170.95	864.59	82.59	9.82

流体包裹体中所保留的原始地质信息失真。为了确保测试结果能准确反映原始卤水成分,应保证所测试的对象为原生石盐流体包裹体,并且未受到后期埋藏变化所带来的影响。单个原生石盐流体包裹体通常为负立方体晶格,常以人字形和堆积形的形式呈面状分布,同时呈现出明暗相间的特征,并且绝大部分流体包裹体的大小十分接近。而次生石盐流体包裹体的形态不规则,主要以脉状或曲线排列的形式存在于石盐晶体的节理缝或裂隙中(Lowenstein and Hardie, 1985; Hardie *et al.*, 1985; Roberts and Spencer, 1995)。石盐流体包裹体在受到后期埋藏改造后,其

原始形态、大小将会发生改变(赵艳军等, 2016; Ding, 2018)。通过显微镜下的岩相学观察,发现ZK0303井石盐中存在大量的原生流体包裹体,主要以单一液相为主,同时也存在少量气液两相的流体包裹体(图3a、3b)。流体包裹体呈正方体或长方体,大小多在30~100 μm之间,偶见大于120 μm的包裹体。流体包裹体组合以人字形和堆积形为主。本次研究所选取的测试对象均为具有原生结构的石盐流体包裹体(图3a、3b),以反映盐湖卤水的真实信息,同时保证流体包裹体在形态、大小方面相一致(图3c、3d),以保证所测数据没有受到后期埋藏所引起的改变。

4.2 江陵凹陷西南部古盐湖卤水演化

ZK0303井在480 m至500 m的范围内沉积了5层石盐,其中的3层原生流体包裹体被保留下来。根据激光剥蚀测试,共获取了包裹体中Li、K、Mg、Ca、Br5种元素的浓度。在石盐形成过程中,CaSO₄的蒸发与沉淀完全带走了卤水中的硫酸根并使得Ca的浓度过量,因此石盐流体包裹体中所保存的卤水为Na-K-Mg-Ca-Cl型(Khmelevska *et al.*, 2000; Galamay *et al.*, 2003; Petrychenko *et al.*, 2005; Kovalevych

et al., 2006; Shen *et al.*, 2017)。在25℃下相对于石盐饱和的Jänecke图(Mg-Ca-2K)中(图5),ZK0303井石盐流体包裹体数据的投点均位于钾石盐沉积的区域,远离含Ca和Mg的蒸发岩矿物沉积区域,比如光卤石、南极石、溢晶石和水氯镁石,这表明江陵凹陷西南部始新世盐湖已达到钾石盐沉积的阶段但未达到光卤石沉积的阶段。

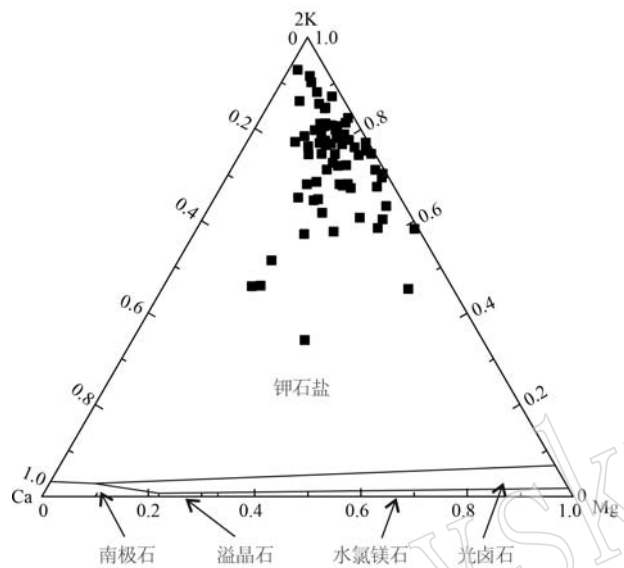


图5 ZK0303井石盐流体包裹体化学成分在25℃下相对于岩盐饱和的Mg-Ca-2K(离子浓度, mol/L)Jänecke图的分布(据Eugster *et al.*, 1980)

Fig. 5 Chemical compositions of halite fluid inclusions from the well ZK0303 in the Mg-Ca-2K Jänecke diagram saturated with respect to halite at 25°C (modified after Eugster *et al.*, 1980)

在图6中可以看到,从下至上,第3组和第1组石盐层中各离子浓度均有所上升。其中,第3组石盐层中Li的浓度由0.85 mg/L升至4.66 mg/L,K的浓度由864.59 mg/L升至1 104.09 mg/L,Mg的浓度由170.95 mg/L升至344.47 mg/L,Br的浓度由9.82 mg/L升至49.82 mg/L,Ca的浓度由82.59 mg/L升至201.04 mg/L;第1组石盐层中Li的浓度由1.05 mg/L升至1.94 mg/L,K的浓度由489.50 mg/L升至1 050.13 mg/L,Mg的浓度由141.74 mg/L升至205.13 mg/L,Br的浓度由22.09 mg/L升至33.20 mg/L,Ca的浓度由209.30 mg/L升至218.09 mg/L。相比于第1组和第3组石盐层各离子浓度,第2组石盐层流体包裹体5种元素的变化范围要高出许多。其中,Li的浓度由6.85 mg/L升至15.10 mg/L,K的浓度由2 168.44 mg/L升至

3 362.15 mg/L,Mg的浓度由725.97 mg/L升至1 448.54 mg/L,Br的浓度由35.33 mg/L升至98.58 mg/L,不同于第1组和第3组石盐层,第2组石盐层中Ca的浓度由417.34 mg/L降低至139.07 mg/L。卤水或蒸发岩矿物中的Br是反映盐湖卤水蒸发程度和阶段的重要指标,其值越高通常表明盐湖蒸发越强,也使得卤水浓度越大(Sanders, 1991; Warren, 2006; Farid *et al.*, 2013; Biehl *et al.*, 2014)。Mg也可以作为指示盐湖卤水浓度的指标,其值越高说明盐湖卤水浓度越大(王海雷等, 2010; Li *et al.*, 2021)。从图5中3组石盐层流体包裹体的离子含量变化可以看到,第2组石盐层中Br和Mg的含量最高,说明该时期盐湖经历了更强的蒸发,导致卤水浓度更大,钾锂的富集程度也更高。

4.3 江陵凹陷西南部古盐湖卤水钾锂来源

ZK0303井第2组石盐层石盐流体包裹体中Li的均值浓度最高达到了15.10 mg/L,K的均值浓度最高达到了3 362.15 mg/L。不过与柴达木盆地一里坪石盐流体包裹体的Li(17.78~193.02 mg/L)和K(1 494.79~11 485.33 mg/L)浓度相比(胡宇飞等, 2021),江陵凹陷西南部始新世盐湖卤水的Li和K浓度仍较低。柴达木盆地盐湖中Li很可能来自于早期蒸发岩的溶解、深层地下水、富锂岩石的低温风化以及淡水的混合(He *et al.*, 2020),而K则主要来自于硅酸盐的风化(Zhang *et al.*, 2019)。

江陵凹陷部分卤水中检测出Ca、F以及一些金属元素(Fe、Mn、Cu、Pb、Cr、Ni、Zn、Ag)等,这与海水的组成成分差别很大,表明卤水可能接受了深部物质的补给(刘成林, 2013; 王春连等, 2013a, 2018)。现代盐湖矿床中硼、锂、铷、铯等微量元素的富集通常与火山热液补给和深部熔融的花岗岩有关(赵元艺等, 2007; Araoka *et al.*, 2014; Yu *et al.*, 2015; 刘成林等, 2016; 王春连等, 2018)。根据Wang等(2017)对凹陷内卤水中Li同位素的分析,认为火山岩中Li是以水-岩反应的方式进入卤水中而不是依靠风化作用。Yu等(2021)在分析了江陵凹陷卤水中H、O、Li、B、Sr等同位素的变化特征后认为,凹陷的富钾锂卤水来自于盐湖卤水,之后的埋藏过程中与储层中的碎屑岩以及火山岩发生了水-岩反应,促使钾锂元素在卤水中富集。Wang等(2022)以凹陷内古新世和始新世的玄武岩为研究对象,进行了不同溶液和温度下的水-岩反应,认为玄武岩在高温

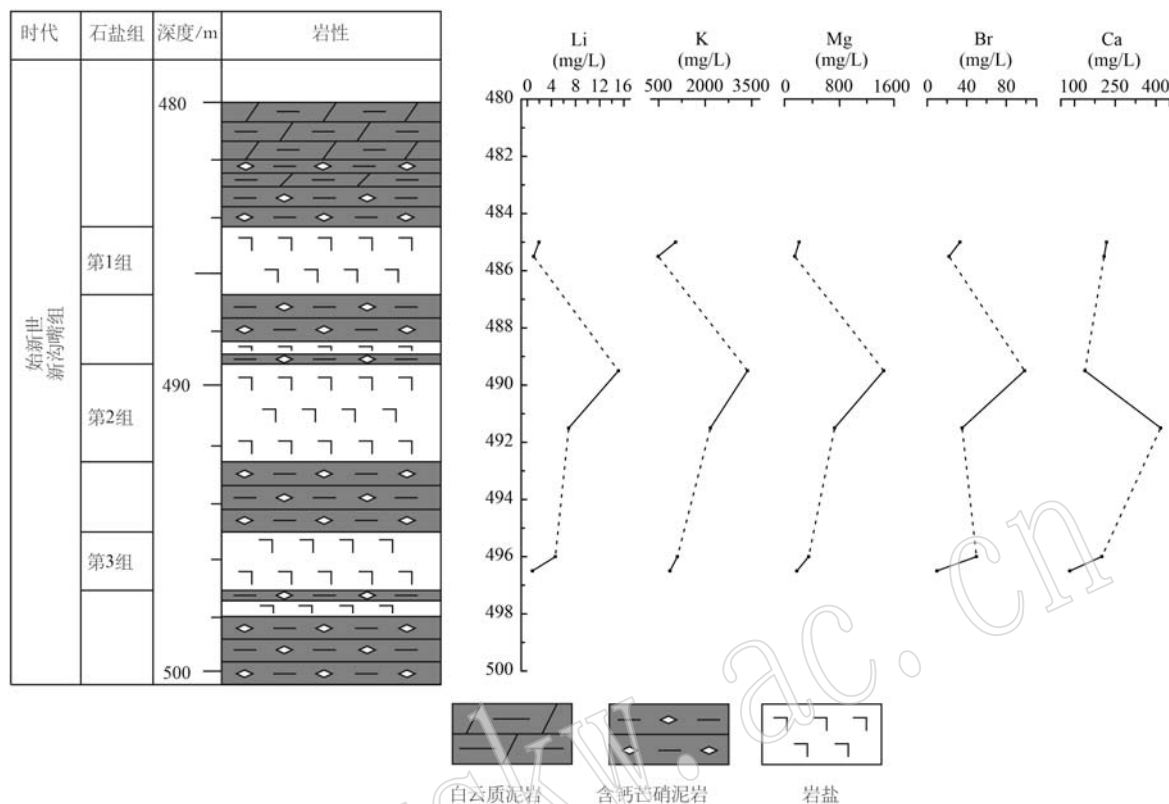


图 6 ZK0303 井流体包裹体化学成分

Fig. 6 Chemical compositions of fluid inclusions in well ZK0303

(250~300 °C)下与卤水的水岩反应是盆地卤水中钾锂富集的主要形式。

前人的研究表明,凹陷内的玄武岩是卤水中钾锂的主要来源。凹陷西南部地层主要以粉砂岩、泥岩以及蒸发岩为主,距离凹陷内的玄武岩分布区较远(图1b)。因此,玄武岩很难为凹陷西南部的盐湖卤水提供足够的钾锂元素。在含蒸发岩的盆地中通常会发生蒸发岩的溶解,从而导致石盐流体包裹体中K的浓度大于Ca和Mg的浓度(Taberner *et al.*, 2000; Timofeeff *et al.*, 2001; Shen *et al.*, 2017)。ZK0303井石盐流体包裹体中Mg、Ca的浓度小于K的浓度,这或许表明江陵凹陷西南部盐湖卤水溶解了早期沉积的蒸发岩从而导致钾的富集。ZK0303井第1组和第3组石盐流体包裹体中Li的均值浓度(0.85~4.66 mg/L和1.06~1.84 mg/L)与海水蒸发至石盐开始沉淀的阶段相似(陈郁华, 1983),但是第2组石盐流体包裹体中Li的均值浓度(6.85~15.10 mg/L)远大于海水蒸发至石盐开始沉淀的阶段,这说明除了蒸发外,Li仍有其他的来源。Zhu等(2023)认为江陵凹陷内的岩盐溶解为地下水提供

了大量的Li元素,继而改变了长江水中 $\delta^7\text{Li}$ 值。Yan等(2023)认为凹陷内始新统卤水中的Li来自于石盐的溶解。因此,江陵凹陷西南部始新世盐湖卤水中锂的富集与钾一样,可能与早期沉积的岩盐被溶解有关。

5 结论

(1) 江陵凹陷西南部始新世石盐流体包裹体所保存的卤水为Na-K-Mg-Ca-Cl型,K的浓度最高达到3 362.15 mg/L, Li的浓度最高达到15.10 mg/L;

(2) 江陵凹陷始新世盐湖卤水的蒸发经历了由低升高再降低的变化,但是均达到钾石盐沉积阶段;

(3) 江陵凹陷西南部始新世盐湖卤水中钾锂的来源除蒸发外,还接受了早期岩盐溶解的贡献。

References

- Araoka D, Kawahata H, Takagi T, *et al.* 2014. Lithium and strontium isotopic systematics in playas in Nevada, USA: Constraints on the origin of lithium[J]. Mineralium Deposita, 49(3): 371~379.

- Benison K C and Goldstein R H. 1999. Permian paleoclimate data from fluid inclusions in halite [J]. *Chemical Geology*, 154(1~4) : 113~132.
- Biehl B C, Reuning L, Strozyk F, et al. 2014. Origin and deformation of intra-salt sulphate layers: An example from the Dutch Zechstein (Late Permian) [J]. *International Journal of Earth Sciences*, 103(3) : 697~712.
- Chen Yuhua. 1983. Sequence of salt separation and regularity of some trace elements distribution during isothermal evaporation (25°C) of the huanghai sea water[J]. *Acta Geoloica Sinica*, 4: 379~390 (in Chinese with English abstract).
- Chu Cheng. 1983. Discussion on the origin of gypsum salts in Xiangli salt mine[J]. *Hunan Geology*, 2(2) : 44~52 (in Chinese with English abstract).
- Ding T. 2018. Evaporation stage of paleo-saline lake in north Shanxi salt basin China: Insight from fluid inclusions in halite[J]. *Carbonates and Evaporites*, 33: 275~283.
- Dong Juan, Gao Xiang, Fang Qinfang, et al. 2015. The characteristics of halite inclusions in the Mengyejing potash deposit, Yunnan Province, and their palaeoenvironmental significance[J]. *Acta Petrologica et Mineralogica*, 34(2) : 227~236 (in Chinese with English abstract).
- Eugster H P, Harvie C E and Weare J H. 1980. Mineral equilibria in a six-component seawater system, Na-K-Mg-Ca-SO₄-Cl-H₂O, at 25°C [J]. *Geochimica et Cosmochimica Acta*, 44(9) : 1 335~1 347.
- Fang Zhixiong. 2006. Sedimentary Filling Model of Jianghan Saline Lake Basin[M]. Beijing: Petroleum Industry Publishing House (in Chinese).
- Farid I, Trabelsi R, Zouari K, et al. 2013. Hydrogeochemical processes affecting groundwater in an Irrigated Land in Central Tunisia[J]. *Environmental Earth Sciences*, 68(15) : 1 215~1 231.
- Frezzotti M L, Tecce F and Casagli A. 2012. Raman spectroscopy for fluid inclusion analysis[J]. *Journal of Geochemical Exploration*, 112(1) : 1~20.
- Galamay A, Bukowski K and Czapowski G. 2003. Chemical composition of brine inclusions in halite from clayey salt (zuber) facies from the Upper Tertiary (Miocene)[J]. *Journal of Geochemical Exploration*, 78-79: 509~511.
- Ghazi A M and Stephen S. 2000. Trace element determination of single fluid inclusions by laser ablation ICP-MS, Applications for halites from sedimentary basins[J]. *The Analyst*, 125(1) : 205~210.
- Gilder S A, Keller G R, Luo M, et al. 1991. Eastern Asia and the Western Pacific timing and spatial distribution of rifting in China[J]. *Tectonophysics*, 197(2~4) : 225~243.
- Hardie L A, Lowenstein T K and Spencer R J. 1985. The problem of distinguishing between primary and secondary features in evaporates [C]//Schreiber B C and Harber H I. Sixth International symposium on Salt. Alexandria, Virginia, USA: Tha Salt Institute, 11~39.
- He M Y, Luo C G, Yang H J, et al. 2020. Sources and a proposal for comprehensive exploitation of lithium brine deposits in the Qaidam Basin on the northern Tibetan Plateau, China: Evidence from Li isotopes[J]. *Ore Geology Reviews*, 117: 103277.
- Hu Mingyue, He Hongliao, Zhan Xiuchun, et al. 2008. Matrix normalization for In-situ multi-element quantitative analysis of zircon in laser ablation-inductively coupled plasma mass spectrometry [J]. *Chinese Journal of Analytical Chemistry*, 36(7) : 947~953 (in Chinese with English abstract).
- Hu Yufei, Wang Mingquan, Zhao Yanjun, et al. 2021. The variations of brine composition and its significance in the Yiliping area of the Qaidam basin—Evidence from fluid inclusions in halite analysed by LA-ICP-MS[J]. *Acta Geologica Sinica*, 95(7) : 2 109~2 120 (in Chinese with English abstract).
- Khmelevska O, Kovalevych V and Peryt T M. 2000. Changes of seawater composition in the Triassic-Jurassic time as recorded by fluid inclusions in halite[J]. *Journal of Geochemical Exploration*, 69: 83~86.
- Kovalevych, V M, Peryt, T M, Zhang, W L, et al. 2006. Composition of brines in halite-hosted fluid inclusions in the Upper Ordovician, Canning Basin, Western Australia: New data on seawater chemistry [J]. *Terra Nova*, 18(2) : 95~103.
- Li J H, Dong S W, Yin A, et al. 2015a. Mesozoic tectonic evolution of the Daba Shan Thrust Belt in the southern Qinling orogen, central China: Constraints from surface geology and reflection seismology [J]. *Tectonics*, 34(8) : 1 545~1 575.
- Li J, Zhang X Y, Hu M Y, et al. 2021. Halogenases of Qarhan salt lake in the Qaidam Basin: Evidence from halite fluid inclusions[J]. *Frontiers in Earth Science*, 9: 698229.
- Li X Y, Zhu P M, Kusky T M, et al. 2015b. Has the Yangtze craton lost its root? A comparison between the North China and Yangtze cratons [J]. *Tectonophysics*, 655: 1~14.
- Liu Chenglin. 2013. Characteristics and formation of potash deposits in continental rift basins: A review[J]. *Acta Geoscientica Sinica*, 34(5) : 515~527 (in Chinese with English abstract).
- Liu Chenglin, Yu Xiaocan, Zhao Yanjun, et al. 2016. A tentative discussion on regional metallogenic background and mineralization mechanism of subterranean brines rich in potassium and lithium in South China Block[J]. *Mineral Deposits*, 35(6) : 1 119~1 143 (in Chinese with English abstract).
- Liu Jinlei, Wang Chunlian, Liu Chenglin, et al. 2015. Geochemical characteristic of the Shashi Formation in Sha 3 well of the Jiangling Depression and its indication for potash formation[J]. *Acta Geologica Sinica*, 89(11) : 2 196~2 202 (in Chinese with English abstract).

- Liu M, Cui X J and Liu F T. 2004. Cenozoic rifting and volcanism in eastern China: A mantle dynamic link to the Indo-Asian collision? [J]. *Tectonophysics*, 393(1~4): 29~42.
- Liu Qingmin and He Liezhen. 1982. Sedimentary characteristics and formation conditions of rock salt deposits in Qingjiang Basin[J]. *China Well and Rock Salt*, 1: 13~17 (in Chinese with English abstract).
- Liu Xingqi and Ni Pei. 2005. Advances in studies of fluid inclusions in halite formed in earth's surface environments[J]. *Advance in Earth Sciences*, 20(8): 856~862 (in Chinese with English abstract).
- Longerich H P, Jackson S E, Gunther D, et al. 1996. Laser ablation inductively coupled plasma-mass spectrometric transient signal data acquisition and analyte concentration calculation[J]. *Journal of Analytical Atomic Spectrometry*, 11(9): 899~904.
- Lowenstein T K and Hardie L A. 1985. Criteria for the recognition of salt-pan evaporates[J]. *Sedimentology*, 32: 627~644.
- Lowenstein T K, Timofeeff M N, Brennan S T, et al. 2001. Oscillations in phanerozoic seawater chemistry: Evidence from fluid inclusions [J]. *Science*, 294(5 544): 1 086~1 088.
- Peng Touping, Wang Yuejun, Fan Weiming, et al. 2006. ^{39}Ar - ^{40}Ar geochronology and geochemistry of the early Tertiary basaltic rocks in the Jianghan basin, China and its petrogenesis[J]. *Acta Petrologica Sinica*, 22(6): 1 617~1 626 (in Chinese with English abstract).
- Petrychenko O Y, Peryt T M and Chechel E I. 2005. Early Cambrian seawater chemistry from fluid inclusions in halite from Siberian evaporites[J]. *Chemical Geology*, 219(1~4): 149~161.
- Roberts S M and Spencer R J. 1995. Paleotemperatures preserved in fluid inclusions in halite [J]. *Geochimica et Cosmochimica Acta*, 59(19): 3 929~3 942.
- Sanders L L. 1991. Geochemistry of formation waters from the lower Silurian Clinton Formation (Albion Sandstone), eastern Ohio[J]. *The American Association of Petroleum Geologists Bulletin*, 75(10): 1 593~1 608.
- Shen C B, Donelick R A, O'Sullivan P B, et al. 2012. Provenance and hinterland exhumation from LA-ICP-MS zircon U-Pb and fission-track double dating of Cretaceous sediments in the Jianghan Basin, Yangtze block, central China[J]. *Sedimentary Geology*, 281: 194~207.
- Shen Lijian, Liu Chenglin, Xu Haiming, et al. 2014. Paleocene mineral assemblage characteristics of Jiangling Depression and their significance for potash formation[J]. *Mineral Deposits*, 33(5): 1 020~1 030 (in Chinese with English abstract).
- Shen Lijian, Liu Chenglin, Wang Licheng, et al. 2017. Degree of brine evaporation and origin of the Mengyejing potash deposit: Evidence from fluid inclusions in halite[J]. *Acta Geologica Sinica (English Edition)*, 91(1): 175~185.
- Shepherd T J, Ayora C, Cendón D I, et al. 1998. Quantitative solute analysis of single fluid inclusions in halite by LA-ICP-MS and cryo-SEM-EDS: Complementary microbeam techniques [J]. *European Journal of Mineralogy*, 10(6): 1 097~1 108.
- Shepherd T J, Naden J, Chereny S R, et al. 2000. Chemical analysis of palaeogroundwaters: A new frontier for fluid inclusion research [J]. *Journal of Geochemical Exploration*, 69: 415~418.
- Sun X H, Hu M Y, Liu C L, et al. 2013. Composition determination of single fluid inclusions in salt minerals by Laser Ablation ICP-MS[J]. *Chinese Journal of Analytical Chemistry*, 41(2): 235~241.
- Sun Xiaohong, Hu Yufei, Liu Chenglin, et al. 2016. Argument that brine of salty lake in Sichuan basin had reached crystallizing point of potash minerals during Triassic: Evidence from chemical composition of fluid inclusions in halite[J]. *Minerals Deposits*, 35(6): 1 157~1 168 (in Chinese with English abstract).
- Taberner C, Cendón D I, Pueyo J J, et al. 2000. The use of environmental markers to distinguish marine vs. continental deposition and to quantify the significance of recycling in evaporite basins[J]. *Sedimentary Geology*, 137(3~4): 213~240.
- Teng X H, Fang X M, Kaufman A J, et al. 2019. Sedimentological and mineralogical records from drill core SKD1 in the Jianghan Basin, Central China, and their implications for late Cretaceous-early Eocene climate change[J]. *Journal of Asian Earth Sciences*, 182: 103936.
- Timofeeff M N, Lowenstein T K, Brennan S T, et al. 2001. Evaluating seawater chemistry from fluid inclusions in halite: Examples from modern marine and nonmarine environments[J]. *Geochimica et Cosmochimica Acta*, 65(14): 2 293~2 300.
- Timofeeff M N, Lowenstein T K, Da Silva M A M, et al. 2006. Secular variation in the major-ion chemistry of seawater: Evidence from fluid inclusions in Cretaceous halites[J]. *Geochimica et Cosmochimica Acta*, 70(8): 1 977~1 994.
- Wang Chunlian, Liu Chenglin, Xu Haiming, et al. 2013a. Homogenization temperature research of salt inclusion in the upper section of Shashi Formation in Jiangling Depression [J]. *Acta Petrologica et Mineralogica*, 32(3): 383~392 (in Chinese with English abstract).
- Wang Chunlian, Liu Chenglin, Xu Haiming, et al. 2013b. Carbon and oxygen isotopes characteristics of Paleocene saline lake facies carbonates in Jiangling Depression and their environmental significance[J]. *Acta Geoscientica Sinica*, 34(5): 567~576 (in Chinese with English abstract).
- Wang Chunlian, Liu Chenglin, Liu Baokun, et al. 2015. The discovery of carnallite in Paleocene Jiangling Depression and its potash searching significance[J]. *Acta Geologica Sinica*, 89(1): 129~136 (in Chinese with English abstract).
- Wang Chunlian, Huang Hua, Wang Jiuyi, et al. 2018. Geological features and metallogenetic model of K-and Li-rich brine ore field in the

- Jiangling depression[J]. *Acta Geologica Sinica*, 92(8): 1 630~1 646 (in Chinese with English abstract).
- Wang Chunlian, Liu Lihong, Li Qiang, et al. 2020. Petrogeochemical characteristics and genetic analysis of the source area of brine type lithium-potassium ore sources area in Jitai basin of Jiangxi Province [J]. *Acta Petrologica et Mineralogica*, 39(1): 65~84 (in Chinese with English abstract).
- Wang Chunlian, Meng Lingyang, Liu Chenglin, et al. 2021. A study of the genesis of Paleocene underground brine deposits in Jiangling depression[J]. *Acta Petrologica et Mineralogica*, 40(1): 1~13 (in Chinese with English abstract).
- Wang Chunlian, Yu Xiaocan, Li Ruiqin, et al. 2022. Origin of lithium-potassium-rich brines in the Jianghan Basin, South China: Constraints by water-rock reactions of Mesozoic-Cenozoic igneous rocks [J]. *Minerals*, 11(12): 1 330.
- Wang Hailei and Wang Yunsheng. 2010. Preliminary analysis on Mg^{2+} , Ca^{2+} and Mg/Ca as salinity indicators of lakes in the Qinghai-Tibetan Plateau[J]. *Journal of Lake Sciences*, 22(6): 849~900 (in Chinese with English abstract).
- Wang L C, Liu C L, Wang C L, et al. 2017. Lithium isotope evidence for the source of potassium-rich brine solutes in the Jiangling depression of central China[J]. *Acta Geologica Sinica* (English edition), 91(1): 363~364.
- Warren J K. 2006. *Evaporites: Sediments, Resources and Hydrocarbons* [M]. Berlin: Springer-Verlag Berlin Heidelberg.
- Wu L L, Mei L F, Liu Y S, et al. 2017. Multiple provenance of rift sediments in the composite basin-mountain system: Constraints from detrital zircon U-Pb geochronology and heavy minerals of the early Eocene Jianghan Basin, central China[J]. *Sedimentary Geology*, 349: 46~61.
- Wu L L, Mei L F, Douglas A P, et al. 2020. Basement structures have crucial influence on rift development: Insights from the Jianghan Basin, central China[J]. *Tectonics*, 39: e2019TC005671.
- Xi Binbin, Qian Yixiong, Shi Weijun, et al. 2015. The characteristics of primary inclusions in halite in Bachu Uplift of Tarim Basin and their implications for paleo-temperature: A case study of well Bt5[J]. *Acta Petrologica et Mineralogica*, 34(1): 79~86 (in Chinese with English abstract).
- Xu Lunxun, Yan Chunde, Yu Huilong, et al. 1995. Chronology of Paleogene volcanic rocks in Jianghan Basin[J]. *Oil Gas Geology*, 16(2): 132~137 (in Chinese with English abstract).
- Xu Yang, Cao Yangtong and Liu Chenglin, et al. 2018. Provenance and degree of evaporation and concentration of Eocene salt lake in the Kuqa Basin[J]. *Acta Geologica Sinica*, 92(8): 1 617~1 629 (in Chinese with English abstract).
- Xu Yang, Cao Yangtong and Liu Chenglin. 2021. Brine temperature of early Eocene salt formation period in Kuqa Basin and its significance [J]. *Editorial Committee of Earth Science—Journal of China University of Geosciences*, 46(11): 4 188~4 196 (in Chinese with English abstract).
- Xu Y, Cao Y T and Liu C L. 2021a. Mid-Eocene sea surface cooling in the easternmost proto-Paratethys sea: Constraints from quantitative temperatures in halite fluid inclusions[J]. *International Journal of Earth Sciences*, 110(7): 1 713~1 727.
- Xu Y, Cao Y T and Liu C L. 2021b. Whether the middle Eocene salt-forming brine in the Kuqa Basin reached the potash-forming stage: Quantitative evidence from halite fluid inclusions[J]. *Geofluids*, (2): 1~12.
- Yan K, Wang C L, Liu C L, et al. 2022. Reconstruction of early Paleogene landscapes and climate in the Jianghan Basin, central China: Evidence from evaporites and palynology[J]. *Palaeogeography, Palaeoclimatology, Palaeoecology*, 601: 111095.
- Yan K, Wang C L, Chen R Y, et al. 2023. Origin and evolution of deep lithium-rich brines in the southwest Jianghan Basin, central China: Evidence from hydrochemistry and stable isotopes[J]. *Journal of Hydrology*, 626: 130163.
- Yang Jigen. 1994. The preliminary study of fluid inclusion in salt from five halite deposits of four Provinces in southeast China[J]. *Journal of Salt Lake Science*, 2(3): 1~9 (in Chinese with English abstract).
- Yao Qiuchang and Lou Jisheng. 2008. Analysis of hydrocarbon accumulation conditions in Yuanjiang Sag of Dongting Basin[J]. *Natural Gas Industry*, 28(9): 37~40 (in Chinese with English abstract).
- Yu X C, Wang C L, Liu C L, et al. 2015. Sedimentary characteristics and depositional model of a Paleocene-Eocene salt lake in the Jiangling Depression[J]. *Chinese Journal of Oceanology and Limnology*, 33(6): 1 426~1 435.
- Yu X C, Liu C L, Wang C L, et al. 2021. Origin of geothermal waters from the upper Cretaceous to lower Eocene strata of the Jiangling Basin, South China: Constraints by multi-isotopic tracers and water-rock interactions[J]. *Applied Geochemistry*, 124: 104810.
- Yu Xinqi, Shu Liangshu, Deng, Ping, et al. 2003. The sedimentary features of the Jurassic-Tertiary terrestrial strata in southeast China[J]. *Journal of Stratigraphy*, 27(3): 224~263 (in Chinese with English abstract).
- Yuan Jianqi, Cai Keqin, Xiao Rongge, et al. 1991. The characteristics and genesis of inclusions in salt from Mengyejing potash deposit in Yunnan Province[J]. *Earth Science—Journal of China University of Geosciences*, 16(2): 137~142 (in Chinese with English abstract).
- Zhang X R, Fan Q S, Li Q K, et al. 2019. The source, distribution, and

- sedimentary pattern of K-rich brines in the Qaidam Basin, western China[J]. Minerals, 9(11): 655.
- Zhao Yanjun, Liu Chenglin and Hu Yufei. 2016. Sedimentary environment and sedimentation of evaporate in the fifth Member of Majiagou Formation of Salt Basin in northern Shaanxi Ordovician strata: Evidence from fluid inclusions[J]. Mineral deposits, 35(6): 1 144~1 156 (in Chinese with English abstract).
- Zhao Yuanyi, Lie Fengjun, Hou Zengqian, et al. 2007. Geochemistry of Targejia hot spring type cesium deposit in Tibet[J]. Mineral Deposits, 25(2): 163~174 (in Chinese with English abstract).
- Zhu Guanhong, Ma Jinlong, Wei Gangjian, et al. 2023. Lithium isotope fractionation during the weathering of granite: Response to pH[J]. Geochimica et Cosmochimica Acta, 345: 117~119.

附中文参考文献

- 陈郁华. 1983. 黄海水25℃恒温蒸发时的析盐序列及某些微量元素的分布规律[J]. 地质学报, 4: 379~390.
- 储澄. 1983. 湘澧盐矿的膏盐类矿物成因探讨[J]. 湖南地质, 2(2): 44~52.
- 董娟, 高翔, 方勤方, 等. 2015. 云南勐野井钾盐矿床石盐包裹体特征及古环境意义[J]. 岩石矿物学杂志, 34(2): 227~236.
- 方志雄. 2006. 江汉盆地盐湖沉积充填模式[M]. 北京: 石油工业出版社.
- 胡明月, 何红蓼, 詹秀春, 等. 2008. 基体归一定量技术在激光烧蚀-等离子体质谱法锆石原位多元素分析中的应用[J]. 分析化学, 36(7): 947~953.
- 胡宇飞, 汪明泉, 赵艳军, 等. 2021. 柴达木盆地一里坪盐湖成盐卤水成分变化及其意义——来自LA-ICP-MS分析石盐流体包裹体组成的证据[J]. 地质学报, 95(7): 2 109~2 120.
- 刘成林. 2013. 大陆裂谷盆地钾盐矿床特征与成矿作用[J]. 地球学报, 34(5): 515~527.
- 刘成林, 余小灿, 赵艳军, 等. 2016. 华南陆块液体钾、锂资源的区域成矿背景与成矿作用初探[J]. 矿床地质, 35(6): 1 119~1 143.
- 刘锦磊, 王春连, 刘成林, 等. 2015. 江陵凹陷沙钾3井古近系沙市组地球化学特征及成钾指示[J]. 地质学报, 89(11): 2 196~2 202.
- 刘庆民, 何烈珍. 1982. 清江盆地岩盐矿床沉积特征与形成条件[J]. 中国井矿盐, 1: 11~15.
- 刘兴起, 倪培. 2005. 表生环境条件形成的石盐流体包裹体研究进展[J]. 地球科学进展, 20(8): 856~862.
- 彭头平, 王岳军, 范蔚茗, 等. 2006. 江汉盆地早第三纪玄武质岩石³⁹Ar/⁴⁰Ar年代学和地球化学特征及其成因意义[J]. 岩石学报, 22(6): 1 617~1 626.
- 沈立建, 刘成林, 徐海明, 等. 2014. 江陵凹陷古新统盐类矿物沉积特征及其成钾指示意义[J]. 矿床地质, 33(5): 1 020~1 030.
- 孙小虹, 胡宇飞, 刘成林, 等. 2016. 四川盆地三叠纪古盐湖已达钾盐析出阶段—来自石盐流体包裹体化学组成的约束[J]. 矿床地质, 35(6): 1 157~1 168.
- 王春连, 刘成林, 徐海明, 等. 2013a. 江陵凹陷沙市组上段石盐包裹体测温学研究[J]. 岩石矿物学杂志, 32(3): 383~392.
- 王春连, 刘成林, 徐海明, 等. 2013b. 江陵凹陷古新世盐湖沉积碳酸盐碳氧同位素组成及其环境意义[J]. 地球学报, 34(5): 567~576.
- 王春连, 刘成林, 刘宝坤, 等. 2015. 江陵凹陷古新统光卤石的发现及其钾盐找矿意义[J]. 地质学报, 89(1): 129~136.
- 王春连, 黄华, 王九一, 等. 2018. 江陵凹陷富钾锂卤水矿田地质特征及成藏模式研究[J]. 地质学报, 92(8): 1 630~1 646.
- 王春连, 刘丽红, 李强, 等. 2020. 江西吉泰盆地卤水型锂钾矿物区岩石地球化学特征及成因分析[J]. 岩石矿物学杂志, 39(1): 65~84.
- 王春连, 孟令阳, 刘成林, 等. 2021. 江陵凹陷古新世地下卤水型硼矿床成因研究[J]. 岩石矿物学杂志, 40(1): 1~13.
- 王海雷, 王云生. 2010. 青藏高原湖泊Mg²⁺, Ca²⁺和Mg/Ca盐度指示意义的初步分析[J]. 湖泊科学, 22(6): 894~900.
- 席斌斌, 钱一雄, 施伟军, 等. 2015. 塔里木盆地巴楚隆起岩盐中原生包裹体特征及意义——以巴探5井为例[J]. 岩石矿物学杂志, 34(1): 79~86.
- 徐论勋, 阎春德, 俞惠隆, 等. 1995. 江汉盆地地下第三系火山岩年代[J]. 石油与天然气地质, 16(2): 132~137.
- 徐洋, 曹养同, 刘成林, 等. 2018. 库车盆地始新世盐湖物源及蒸发浓缩程度研究[J]. 地质学报, 92(8): 1 617~1 629.
- 徐洋, 曹养同, 刘成林. 2021. 库车盆地早始新世成盐期卤水温度及其意义[J]. 地球科学, 46(11): 4 188~4 196.
- 杨吉根. 1994. 我国东南四省五个岩盐矿床石盐中流体包裹体的初步研究[J]. 盐湖研究, 2(3): 1~9.
- 姚秋昌, 楼基胜. 2008. 洞庭盆地沅江凹陷油气成藏条件分析[J]. 天然气工业, 28(9): 37~40.
- 余心起, 舒良树, 邓平, 等. 2003. 中国东南部侏罗纪-第三纪陆相地层沉积特征[J]. 地层学杂志, 27(3): 254~263.
- 袁见齐, 蔡克勤, 肖荣阁, 等. 1991. 云南勐野井钾盐矿床石盐中包裹体特征及其成因的讨论[J]. 地球科学, 16(2): 137~142.
- 赵艳军, 刘成林, 胡宇飞. 2016. 陕北盐盆奥陶系马家沟组五段蒸发岩沉积环境与作用——来自石盐流体包裹体的证据[J]. 矿床地质, 35(6): 1 144~1 156.
- 赵元艺, 聂凤军, 侯增谦, 等. 2007. 西藏搭格架热泉型铯矿床地球化学[J]. 矿床地质, 25(2): 163~174.